Quasiparticle band structures and optical spectra of β-cristobalite SiO_2

L. E. Ramos, J. Furthmüller, and F. Bechstedt
Institut für Festkörpertheorie und Theoretische Optik, Friedrich-Schiller-Universität, 07743 Jena, Germany
(Received 9 July 2003; revised manuscript received 16 October 2003; published 13 February 2004)

Band structures and dielectric functions are calculated using density-functional theory and local-density approximation for three β-cristobalite modifications of SiO_2 with space-group symmetries $Fd3m$, $I\bar{4}2d$, and $P2_13$. Quasiparticle corrections for the Kohn-Sham eigenvalues are determined in a GW approach. The fundamental energy gaps, absorption onsets, and dielectric functions are discussed and compared in the light of experimental data and previous calculations.

DOI: 10.1103/PhysRevB.69.085102 PACS number(s): 71.20.Ps, 61.50.Ah, 77.22.Ch, 78.20.Ci

I. INTRODUCTION

The dimensional scaling required for the novel semiconductor devices based on silicon demands more comprehensive investigations of the atomic structure of the surfaces and interfaces involved.[1] As the area of the oxide gate of the metal-oxide-semiconductor transistors decreases and the SiO_2 layer is made thinner, defects at the interface Si/SiO_2 are supposed to play a more important role in the electronic properties.[2–4] Although, there is an ongoing search for alternative high-κ materials, the use of SiO_2 is still essential for the Si-based technology.[5] In addition to the consolidated application of the Si/SiO_2 system in electronic devices, there are also possibilities for optoelectronic applications. The oxidation of porous or amorphous Si is known to affect significantly the luminescence properties observed in these materials.[6] Intense photoluminescence has been detected from Si nanocrystals embedded in SiO_2 and optical gain has recently been reported.[7,8] In order to understand the electronic and optical properties of the various Si/SiO_2 systems, the electronic structure and optical spectra of SiO_2 should be investigated in more detail.

Silicon dioxide or silica may exist in many different crystalline forms, most of them formed by fourfold-coordinated Si and twofold-coordinated O atoms.[9] The structural and electronic properties of these polymorphs have been studied by applying different theoretical and experimental methods.[9–19] Due to the technological importance of polycrystalline or amorphous SiO_2, experimental data for the electronic states of this compound measured by photoemission spectroscopy and similar techniques are available since the early days of semiconductor technology.[20–28]

Structural, bonding, and electronic properties of the ideal β-cristobalite SiO_2 were first investigated theoretically by linear combination of atomic orbitals (LCAO) and extended tight-binding (TB) methods.[29,30] However, these methods require empirical parameters which are often adjusted in order to achieve the correct fundamental gap, for instance. The β-cristobalite structure with space group $Fd3m$ is also a natural choice to model theoretically SiO_2, when studying Si/SiO_2 interfaces, due to its structural simplicity.[2,31–34] The real structure of β-cristobalite is still controversial, and several symmetries whose changes mainly concern the oxygen atomic sites have been proposed in the literature.[16–18,35] Although there are other structural models, the most accepted symmetries of β-cristobalite structures correspond to the space groups $Fd3m$ (face-centered cubic, fcc), $I\bar{4}2d$ (body-centered tetragonal, bt), and $P2_13$ (simple cubic, sc).

The first step towards the theoretical modeling of interfaces and nanostructures is to describe correctly the band-gap region of the bulk materials involved. While methods based on the density-functional theory give rise to good structural parameters, they fail to describe the fundamental gap energies and energetical positions of defect levels, for instance. In the electronic structure and optical properties of SiO_2 polymorphs, studied by usual *ab initio* and other methods, the quasiparticle (QP) character of the excited energy levels is often not taken into account.[9,15,16,18] To our knowledge no band structure for β-cristobalite SiO_2 including quasiparticle corrections has been reported in the literature. Only in a recent calculation of optical properties in α-quartz[36] additional many-body effects have been considered. Despite numerous experimental and theoretical studies on the SiO_2 systems, the optical spectra cannot be considered well understood. Considering the many polytypes of SiO_2, there is a need for calculations of their complete quasiparticle band structures and for the investigation of quasiparticle effects on their optical properties.

In this paper we present *ab initio* calculations of band structures and frequency-dependent dielectric functions for β-cristobalite including quasiparticle shifts. The paper is organized as follows. In Sec. II, the computational methods are described. In Sec. III, we present the calculated basic structural properties, band structures with quasiparticle corrections, and frequency-dependent dielectric functions. Optical transitions and dielectric constants are discussed and compared to the available experimental data. Conclusions are given in Sec. IV.

II. COMPUTATIONAL METHODS

The structural parameters and Kohn-Sham (KS) eigenvalues are calculated in the framework of the density-functional theory[37] and local-density approximation.[38] To describe the exchange and correlation energy per electron, we apply the parametrization of Perdew and Zunger[39] of the quantum Monte Carlo results of Ceperley and Alder.[40] The interaction between electrons and atomic cores is described by means of non-norm-conserving pseudopotentials implemented in the

 ©2004 The American Physical Society

Vienna *ab initio* simulation package.[41,42] The pseudopotentials are generated in accordance to the projector augmented wave (PAW) method.[43,44]

The use of PAW pseudopotentials addresses the problem of the inadequate description of the wave functions in the core region common to other pseudopotential approaches.[45] The application of the PAW method allows us to construct orthonormalized all-electron-like wave functions for the Si $3p$, Si $3s$, O $2p$, and O $2s$ valence electrons under consideration. The wave functions are used to compute the matrix elements of the exchange-correlation (XC) self-energy operator[46] within the quasiparticle approach[47] as well as the optical transition matrix elements.[45] As for the ultrasoft pseudopotentials,[48,49] the cutoff energies of the PAW pseudopotentials remain considerable small, accounting 18 Ry for Si and 29 Ry for O. The higher-energy cutoff of O in comparison to Si requires a general energy cutoff of plane waves in SiO_2 of about 29 Ry.

The lattice constants a of the cubic structures $Fd3m$ and $P2_13$ are determined directly by fitting the curve of total energy versus volume to Murnaghan's equation of state.[50] For the tetragonal $I\bar{4}2d$ structure, first we choose a set of volumes, and for each volume the ratio c/a is optimized obtaining a set of minimum total energies. The structural c and a parameters are determined by fitting this set of minimum total energies and corresponding volumes to Murnaghan's equation. The atomic positions of the three β-cristobalite modifications with their optimal lattice parameters are then relaxed in order to achieve negligible atomic forces.

Eigenvalues obtained by solving the KS equations of the DFT-LDA (where DFT stands for density-functional theory and LDA for local-density approximation) do not describe correctly the excitation energies of electrons or holes. A more accurate description is given by taking the quasiparticle character of electrons and holes into account. The real part of the corresponding XC self-energy, beyond the XC potential used in the DFT-LDA, gives rise to a QP shift and, hence, to a new eigenvalue for a given band and a given **k** point in the Brillouin zone (BZ).[47] In order to determine the band structure with quasiparticle corrections, first we perform self-consistent calculations within DFT-LDA, obtaining KS eigenvalues along the high-symmetry lines in the Brillouin zone. Second, each DFT-LDA eigenvalue is corrected by a quasiparticle energy shift, the latter calculated according to the GW approximation (G stands for Green's function and W is the screened Coulomb potential) described in Refs. 46 and 47. Within this approximation the quasiparticle self-energy operator can be divided into statically screened and dynamically screened contributions. The quasiparticle energy shifts are in general small, justifying a linear expansion of the self-energy around a DFT-LDA eigenvalue.[51,52] Using an approximate GW version[53] the inverse dielectric function is described by a model function depending on the local electron density. The simplified GW method[53] allows an efficient treatment of the QP corrections for systems with many atoms in the unit cell.[46] To model the dielectric function in the screened potential, we use as an input parameter the electronic dielectric constant of the compound, calculated for vanishing frequency within the independent-particle approximation for the dielectric function.

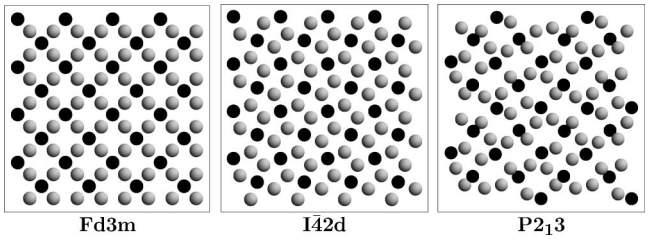

FIG. 1. Atomic structures for three different polymorphs of β-cristobalite. The silicon (oxygen) atoms are represented by black (gray) circles. A projection onto a (001) plane (cubic systems) or (0001) plane (tetragonal SiO_2) is shown.

The frequency-dependent dielectric functions are computed within both the independent-particle picture, using DFT-LDA in a random-phase-like approximation, and the independent-quasiparticle picture, replacing the KS eigenvalues by the ones corrected by QP shifts.[54] The optical matrix elements using PAW pseudopotentials are calculated following the procedure described in Refs. 45 and 55. When QP corrections are included, the optical matrix elements need to be multiplied by the ratio between the QP transition energies and the DFT-LDA transition energies, as observed by Del-Sole and Girlanda.[56] Applying quasiparticle corrections to the energy transitions without the corresponding scaling of the optical matrix elements would lead to more underestimated dielectric constants.[57] The tetrahedron method is applied to calculate the imaginary part of the dielectric function, whereas the real part follows using the Kramers-Kronig relation. The **k**-point mesh used to calculate the dielectric function corresponds to a standard Monkhorst-Pack mesh.[58] The convergence of the spectra with the number of conduction bands and the **k**-point mesh is carefully tested. We consider conduction bands in an energy range of about 100 eV above the lowest state in the valence bands. More than 100 **k** points are used in the irreducible part of the Brillouin zone.

III. RESULTS AND DISCUSSION

A. Structural properties

Projections of the considered SiO_2 structures corresponding to the space groups $Fd3m$, $I\bar{4}2d$, and $P2_13$ are shown in Fig. 1. The ideal β-cristobalite is a diamondlike Si structure with O atoms bridging two Si atoms and corresponds to the space group *Fd3m*. Its primitive unit cell contains two SiO_2 units. The resulting Si-O-Si bond angle of 180° is large and, hence, the Si-O distance is much smaller than in other silica polymorphs. For the two other structures, the arrangement of the silicon atoms is in accordance with the diamond structure, whereas the oxygen atomic sites determine the particular symmetry. The tetragonal polymorph may be considered as a distortional derivative of the ideal fcc structure along a cubic axis. Like the $Fd3m$ structure, the $I\bar{4}2d$ structure is also characterized by one bond length and one Si-O-Si angle. On the other hand, the description of the $P2_13$ structure needs four different bond lengths and Si-O-Si angles.

TABLE I. Lattice constants a and c (in Å), Si-O bond lengths (in Å), bond angles (in deg) and cohesive energies E_{coh} (in eV/SiO_2) for β-cristobalite with space groups $F3dm$, $I\bar{4}2d$, and $P2_13$. The numbers in parentheses indicate inequivalent atoms.

	$F3dm$	$I\bar{4}2d$	$P2_13$
a	7.391	5.095	7.117
c		7.102	
Si(1)-O(1)	1.601	1.609	1.602
Si(1)-O(2)			1.609
Si(2)-O(1)			1.599
Si(2)-O(2)			1.610
O(2)-Si(1)-O(2)	109.5°	107.8°	108.8°
O(1)-Si(1)-O(2)		113.0°	110.2°
O(2)-Si(2)-O(2)			109.9°
O(1)-Si(2)-O(2)			109.0°
Si(1)-O(2)-Si(2)		150.1°	146.7°
Si(1)-O(1)-Si(2)	180.0°		180.0°
E_{coh}	−25.91	−25.93	−25.26

The structural and electronic properties of these three structures have been studied in primitive unit cells, containing two ($Fd3m$), four ($I\bar{4}2d$), and eight SiO_2 units ($P2_13$).

The optimized lattice constants, bond lengths, and cohesive energies per SiO_2 unit are listed in Table I. Our results agree well with those obtained by Demuth and co-workers in a comprehensive investigation on structural properties of silica polymorphs.[9] For the fcc and bt polymorphs the small differences in the lattice constants and cohesive energies can be attributed to the use of the PAW pseudopotentials instead of ultrasoft potentials. The same holds for the bond angles of the sc structure. Deviations of the characteristic bond length and cohesive energies indicate that our optimized sc structure only represents a local minimum on the total-energy surface in comparison to the findings of Demuth and co-workers.[9] However, the optimized geometry for the sc structure is reasonable to discuss the influence of the structures on the electronic structure and optical properties.

For the β-cristobalite symmetries considered, the average Si-O bond lengths do not differ significantly from 1.6 Å.

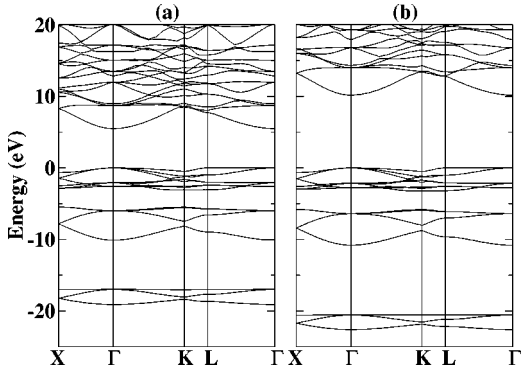

FIG. 2. DFT-LDA (a) and quasiparticle (b) band structures for the symmetry $Fd3m$ of β-cristobalite. The top of valence band coincides with the energy zero.

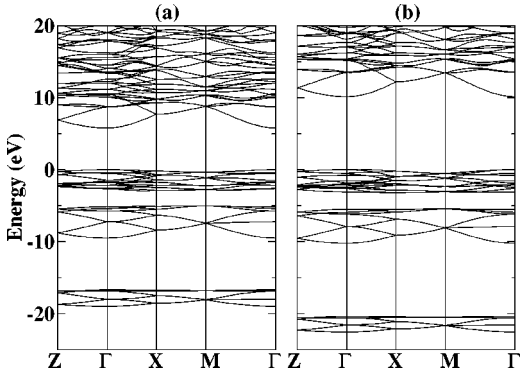

FIG. 3. DFT-LDA (a) and quasiparticle (b) band structures for the symmetry $I\bar{4}2d$ of β-cristobalite. The top of valence band coincides with the energy zero.

This rule is nearly fulfilled by the majority of the SiO_2 polymorphs.[9,10,13–15,18] On the contrary, there is a stronger variation of the average Si-O-Si bond angles in comparison to the ideal value 180° among the symmetries considered. We find 150.1° for $I\bar{4}2d$ and 180° and 146.7° for $P2_13$. On the other hand, the O-Si-O angles deviate only a little in the sc and bt structures when compared to the tetrahedron value 109.47° in the ideal β-cristobalite structure. According to our calculations for the cohesive energy, the tetragonal structure ($I\bar{4}2d$) suggested by O'Keeffe and Hyde[35] is the most stable energetically. For the fcc and bt structures, the trend and the absolute values of our calculated cohesive energies are in agreement with other results obtained by means of *ab initio* methods.[9,18] The sc structure is energetically unfavorable with respect to the others.

B. Electronic structures

The KS band structures (DFT-LDA) and the QP band structures in GW approximation are represented in Figs. 2 −4 for the three SiO_2 polymorphs under consideration. The calculated bands are plotted versus high-symmetry lines in the irreducible parts of the BZ's of the fcc, primitive tetragonal (pt), and sc Bravais lattices. For simplicity, the BZ of a pt structure is used instead of that of a bt lattice.

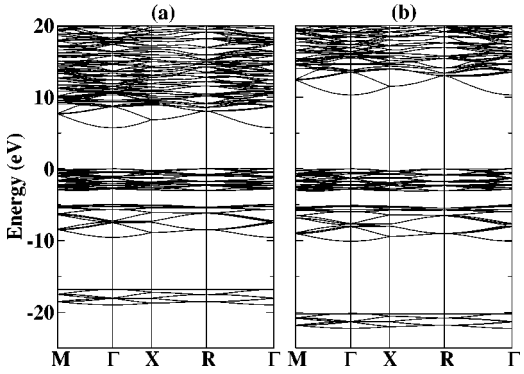

FIG. 4. DFT-LDA (a) and quasiparticle (b) band structures for the symmetry $P2_13$ of β-cristobalite. The top of valence band coincides with the energy zero.

In order to determine the quasiparticle shifts of the Kohn-Sham eigenvalues in our GW approach, the calculation of the dielectric constants ϵ_∞ for the three structures was required. The corresponding dielectric functions computed in the framework of DFT-LDA using primitive unit cells are discussed in Sec. III C. The real part of the corresponding dielectric function $\mathrm{Re}\epsilon(\omega)$ in the independent-particle approximation is used to estimate the dielectric constant ϵ_∞. For the cubic symmetries, $Fd3m$ and $P2_13$, we apply the only independent component of the dielectric tensor, whereas for the tetragonal symmetry $I\bar{4}2d$ we apply an averaged value of the two independent components. In contrast to semiconductors of small gaps, the value of the dielectric constant used has a strong influence on the electronic structure of insulators. In a GW test calculation for the structure $I\bar{4}2d$, we applied a dielectric constant $\epsilon_\infty=2.6$, similar to the ones calculated by Xu and co-workers,[15] instead of the averaged value of the two independent components $\epsilon_\infty=2.27$. The increase of the dielectric constant by 14% gives rise to a variation of the QP fundamental gap from 10.12 eV to 9.62 eV, i.e., to a gap reduction of 5%. The relative influence of the input parameters is the same as for semiconductors, but the absolute variations are obviously larger for insulators such as SiO_2.

Figures 2–4 show three groups of valence bands and the conduction band above the fundamental gap for the three SiO_2 structures. The main features of the band structures are independent of the polymorph and the inclusion of quasiparticle corrections. As for the other 4:2-coordinated SiO_2 systems,[10,11,13,30] the uppermost group of valence bands is mainly derived from nonbinding O $2p$ orbitals filled with two electrons (lone pair). The second group of valence bands is built by O $2p$–Si $3p$ and O $2p$–Si $3s$ bonding orbital combinations (σ states). The third group of valence bands is much lower in energy and formed by nonbinding O $2s$ states. The antibonding orbital combinations O $2p$–Si $3p$ and O $2p$–Si $3s$ (σ^* states) contribute remarkably to the formation of the lowest empty conduction-band states. The lowest conduction bands exhibit a remarkable dispersion with a pronounced minimum at the Γ point. Together with the weak dispersion of the O $2p$-derived uppermost valence bands at the same point, it results in a direct fundamental gap for the β-cristobalite modifications. The direct gap $E_g(\Gamma)$ is smaller than the indirect gaps, $E_g(\mathbf{k})$, between the valence-band maximum (VBM) and the position of the lowest conduction bands at $\mathbf{k}=X,K,L$, $\mathbf{k}=X,M,Z$, and $\mathbf{k}=X,M,R$, respectively, for fcc, pt, and sc. Besides the fundamental energy gap, there are two ionic gaps between the different groups of valence bands at the Γ points. They are the narrow ionic gap $E_{\mathrm{nig}}(\Gamma)$ between the uppermost groups of valence bands as well as the wider ionic gap $E_{\mathrm{wig}}(\Gamma)$ between the bands of σ bonding states and the O $2s$ states. In addition we define two different valence-band widths at Γ. The lowest valence-band widths LW measure the energetical extent of the two uppermost groups of valence bands including the narrow ionic gap $E_{\mathrm{nig}}(\Gamma)$. The total valence-band widths TW also include the lowest O $2s$ lone-pair states and the wider ionic gap $E_{\mathrm{wig}}(\Gamma)$. All these band-structure parameters are listed in Table II for both DFT-LDA and QP approximation.

TABLE II. Band gaps and band widths (in eV) obtained within DFT-LDA and quasiparticle approach of the three different β-cristobalite structures under consideration. The quantities are defined in the text.

	DFT-LDA			QP		
	fcc	pt	sc	fcc	pt	sc
$E_g(\Gamma)$	5.48	5.79	5.73	10.16	10.12	10.31
$E_g(X,X,X)$	8.29	7.70	6.85	13.23	12.20	11.52
$E_g(K,M,M)$	8.50	8.81	7.68	13.41	13.43	12.42
$E_g(L,Z,R)$	7.74	6.89	8.07	12.82	11.36	13.02
$E_{\mathrm{nig}}(\Gamma)$	2.59	2.51	2.18	2.79	2.40	2.27
$E_{\mathrm{wig}}(\Gamma)$	6.89	7.20	7.27	9.75	10.13	10.07
LW	10.10	9.50	9.55	10.81	10.24	10.10
TW	19.10	18.98	18.98	22.60	22.55	22.26

The variation of the band-structure parameters with respect to the ideal β-cristobalite is not significant, even though we compare the band structures corresponding to different primitive cells. The reduction of the average Si-O-Si bond angle slightly opens the DFT-LDA fundamental energy gap by about 0.3 eV. Quasiparticle corrections destroy this clear structural trend. The $E_g(\Gamma)$ gaps are approximately equal for the fcc and pt structures. Only that of the sc geometry is larger by 0.1–0.2 eV, perhaps as a consequence of the computed small lattice constant (cf. Table II). The calculated KS fundamental gaps are rather similar to other results obtained within DFT-LDA.[15] However, other conclusions of other authors are not unanimous with respect to the influence of the polymorph in the fundamental gaps. Discussing many polymorphs of different coordination Xu and Ching[15] concluded that, apparently there is no direct relationship between bond angle and energy gaps and between bond angle and dielectric constants as well. On the other hand, restricting the analysis to the 4:2 coordinated SiO_2 polymorphs a correlation of energy gaps with respect to bond lengths and to bond angles is suggested by Li and Ching in Ref. 13. Since we consider SiO_2 polymorphs which have been derived from the ideal β-cristobalite structure, a clear trend of the fundamental gaps and the other transition energies can hardly be expected. Conversely, in Table II the bandwidths of the second group of the valence bands and ionic gaps, in particular for DFT-LDA, seem to be strongly influenced by the variation of the atomic structure, in particular the bond angles. In the case of the wider ionic gap, the difference between the ideal and nonideal structures is considerably reduced.

The main effect of the quasiparticle approach is the opening of the energy gaps and transition energies between empty and occupied band states. For the ionic material SiO_2 this can be considered a large effect, at least in absolute values.[16] The openings of the fundamental gaps in Table II vary between 4.3 and 4.7 eV, i.e., about 80% of the KS gaps. We observe a weak correlation between average bond angles and quasiparticle corrections of the fundamental energy gaps [4.68 eV (fcc), 4.58 eV (sc), and 4.33 eV (bt)] among the

three symmetry variations considered. In any case, there is no strict correlation with the averaged lattice constant. The influence of the quasiparticle effects on the uppermost groups of valence bands is much weaker than in the case of the fundamental gaps. The ionic gap between O $2p$ lone-pair states and σ bonding states remains practically unchanged. On the other hand, the QP shifts of the lower σ bands enlarge the lower bandwidths LW by 0.5–0.7 eV, and the wider ionic gap between the second and the third group of valence bands is opened by about 3 eV. This is a consequence of the stronger localization of the O $2s$ states, which results in larger QP shifts towards larger binding energies.[59] Those shifts are accompanied by a similar increase of the total valence-band widths TW.

The resemblances of the band structures derived for three modifications of the SiO_2 β-cristobalite are in agreement with findings of other authors. Their calculations[13,15] showed that also the band structures of α-quartz, β-quartz, α-cristobalite, β-cristobalite, and β-tridymite are rather similar, concerning ionic gaps, fundamental energy gaps, and valence-band widths. Therefore, a rough comparison between our calculations and measurements to determine the electronic structure of other SiO_2 polymorphs is justified.[30] The value measured for the fundamental gap varies in the range of 5–12 eV, depending on the experimental technique applied.[25] Weinberg and co-workers[25] measured a gap of 9.3 eV in thermally grown amorphous SiO_2 films. One of the most accepted gap value of 8.9 eV for polycrystalline SiO_2 was determined by photoconductivity measurements.[19] More recent measurements by Nithianandam and Schnatterly[28] extrapolated the results of their inelastic-electron scattering (IES) studies to a fundamental gap of 9.7 eV for amorphous SiO_2. The optical absorption of α-quartz also shows a sharp peak at this energy position.[20,60] The agreement with our predictions of a direct quasiparticle gap of 10.1–10.3 eV for the SiO_2 β-cristobalite is excellent, in particular, taking the experimental and theoretical uncertainties into account. The presence of defects in SiO_2 crystals, the existence of an Urbach tail for amorphous and polycrystalline samples, and other experimental difficulties prevent an accurate and unambiguous gap determination. Although the DFT-LDA calculations underestimate the fundamental gaps with respect to the experimental values, they also underestimate lattice constants which results in slightly larger KS energy gaps. Another source of inaccuracies is the use of the simplified GW approximation for the QP shifts, which in other wide-gap materials leads to an overestimation of the gaps of about 0.2–0.3 eV.[61]

The experimental identification of the valence-band structure is made by means of different methods: ultraviolet photoemission spectroscopy, x-ray photoemission spectroscopy (XPS), electron-energy-loss spectroscopy (EELS), soft-x-ray emission spectroscopy, IES, and reflectance spectroscopy. In the 1970s and 1980s, series of measurements by several groups were performed in order to determine the valence-band states of SiO_2. Apart from their interpretation, the results of those measurements in general agreed very well. By means of photoemission measurements DiStefano and Eastman measured a LW of 11.2 eV for amorphous SiO_2. Despite the tails in the spectra of the amorphous material, this value is only slightly larger than the 10.1–10.8 eV in Table II. The maximum of the XPS emission from the lowest O $2s$ levels, at about 20.2 eV below the VBM, comes close to the upper boundary of the corresponding calculated QP bands. This also holds for the σ bonding bands with energies between 5.5 and 11.2 eV below VBM. Other XPS measurements[24] found a width of the nonbonding O $2p$ derived bands of about 3.3 eV in good agreement with the band structures in Figs. 2–4.

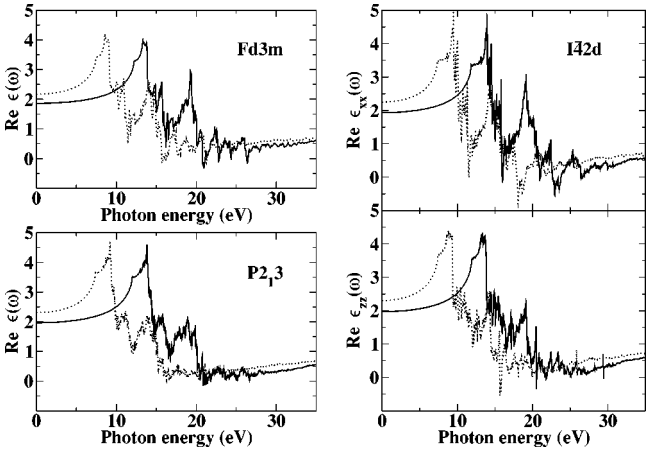

FIG. 5. Real part of the dielectric function of β-cristobalite SiO_2 with the space group $Fd3m$, $I\bar{4}2d$ and $P2_13$, respectively. Solid line, independent-quasiparticle approximation, dotted line, independent-particle approximation. For the tetragonal SiO_2 the two independent tensor components are given.

C. Frequency-dependent dielectric functions

The real and imaginary parts of the dielectric functions calculated for the different β-cristobalite modifications are represented in Figs. 5 and 6. The results obtained within the independent-particle approximation (DFT-LDA) and the

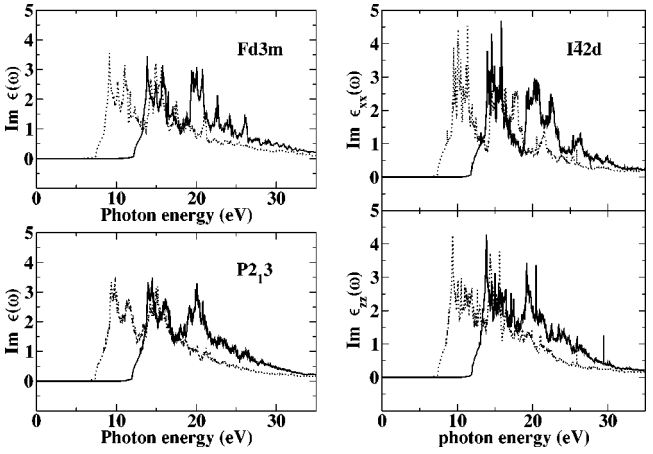

FIG. 6. Imaginary part of the dielectric function of β-cristobalite SiO_2 with the space group $Fd3m$, $I\bar{4}2d$ and $P2_13$, respectively. Solid line, independent-quasiparticle approximation, dotted line, independent-particle approximation. For the tetragonal SiO_2 the two independent tensor components are given.

independent-quasiparticle approach (including QP shifts) are compared. In principle, QP shifts can be calculated for every band and every point in the large **k**-point mesh needed for the calculation of optical properties. However, even when the simplified GW approach is applied, the calculations involved are too time consuming, especially for the sc modification of SiO_2 with 24 atoms in the unit cell. For this reason, we have summarized all QP shifts corresponding to all states and **k** points in three shifts computed by means of the band structures in Figs. 2–4. We have defined three different gap openings Δ_{2p}, Δ_{σ}, and Δ_{2s} for the optical transitions into the conduction bands from the group of valence bands derived from O $2p$ states, σ bonding orbitals, and O $2s$ lone-pair states. The resulting values are $\Delta_{2p}=4.75$ (4.49, 4.62) eV, $\Delta_{\sigma}=5.13$ (4.86, 4.93) eV, and $\Delta_{2s}=8.18$ (7.94, 7.91) eV for $Fd3m$, $I\bar{4}2d$ and $P2_13$, respectively. In practice, three different scissors operators are used depending on the chemical character of the valence bands. We observe two main effects of the QP shifts in the dielectric function. The spectra are shifted towards higher energies and their line shapes, in particular the absorption spectra (proportional to the imaginary parts), remain almost unchanged. However, as a consequence of the widening of the gaps, the amplitude of the real parts of the dielectric functions are slightly reduced by the QP effects.

The real parts of the dielectric functions in Fig. 5 are obtained from a Kramers-Kronig analysis. The zero-frequency limit of Re $\epsilon(\omega)$ gives the static electronic dielectric constant $\epsilon_{\infty}=\mathrm{Re}\,\epsilon(0)$. Within the independent-particle approximation we find $\epsilon_{\infty}=2.17$ and $\epsilon_{\infty}=2.31$, respectively, for the cubic symmetries $Fd3m$ and $P2_13$. The constant $\epsilon_{\infty}=2.17$ is in agreement with the experimental value (see Ref. 29). For the tetragonal symmetry the independent components of the dielectric tensor are $\epsilon_{xx}(0)=2.25$ and $\epsilon_{zz}(0)=2.30$. The inclusion of the QP effects reduce these values to 1.86 ($Fd3m$), 1.97 ($P2_13$), and 1.93 (ϵ_{xx}) and 1.97 (ϵ_{zz}) ($I\bar{4}2d$). Other calculations applying the scissors operator approach and the correction for the optical matrix elements gave rise to underestimated dielectric constants by 10–15% with respect to the DFT-LDA values.[56,57] Similar results for dielectric constants have been found for group-IV semiconductors[61] using a more complete GW approach.[54]

There is a general tendency that the symmetry lowering increases the dielectric constants. However, there is no clear relationship between the variation of the average Si-O-Si bond angle and the dielectric constant. A trend with the reciprocal KS or QP gaps can be hardly derived because of the small variations in energy. In comparison to the values calculated by Xu and Ching[15] using a LCAO method and the values calculated by Pantelides and Harrison using TB,[29] our ϵ_{∞} value for the symmetry $Fd3m$ is smaller. On the other hand, in comparison to the experimental value in Ref. 29 we obtain the value measured for β-cristobalite, at least using DFT-LDA. For the symmetry $Fd3m$, a test calculation applying an oxygen PAW pseudopotential with approximately twice the initial energy cutoff (56 Ry) increases the value of the dielectric constant only by 5%. This reinforces the reliability of the PAW pseudopotentials used in the calculation of optical properties.

The strength of the absorption at energies right above the direct fundamental gaps (see Fig. 6) is vanishing. Therefore, the lowest-energy optical transitions in the β-cristobalite crystals should be forbidden. On the other hand, in vitreous SiO_2 the structural disorder breaks the $\mathbf{k}=0$ selection rule, and optical transitions of any wave-vector transfer should become allowed, at least to some extent. In the QP spectra the first strong peak is observed at about 13.8 eV. Considering a somewhat overestimated peak position, the strong peak at 10.4 eV in the reflectivity[27] could be explained by a strong band-edge exciton with a binding energy of about 3 eV. A discussion based on the tight-binding approach for the complicated interpretation of the band-edge exciton has been given by Laughlin.[26] In a more recent calculation, Chang and co-workers estimated the band-edge exciton energy to be 1.7 eV for α-quartz by solving the Bethe-Salpeter equation.[36]

The tetrahedron method introduces some noise in the curves of dielectric functions, since it does not apply a lifetime broadening. The calculated absorption spectra (Fig. 6) allow us to derive peak positions or, at least, positions of the groups of peaks. We focus our attention to the range of photon energies up to 20 eV and the two cubic geometries. Many peaks occur in the two spectra of the anisotropic tetragonal SiO_2. For $P2_13$ we observe two double peaks at 14.0/14.5 and 18.1/18.6 eV, two broader peaks at 16.1 and 19.3 eV, and a structure centered at 20.2 eV. In the ideal β-cristobalite case, one finds three main structures at 13.9, 15.9, and 19.6/20.1 eV. There are smaller peaks in-between at 15.0, 16.6, 17.1 at 18.9 eV. A direct comparison with experimental data derived from optical or energy-loss spectra is difficult since excitonic effects are not taking into account in the calculations.[36] Measurements of peaks resulted directly from optical reflectance or electron energy-loss spectra may be shifted against the absorption peaks in a nonideal insulator. In addition, the experiments usually are mainly restricted to amorphous SiO_2 or crystalline quartz. This holds for the peak positions 10.3, 11.7, 14.3, and 17.3 eV seen in reflectivity spectra.[20] They are similar to the positions of peaks and shoulders at 10.6, 12.5, 14.5, and 17.8 eV in inelastic electron-scattering spectra of amorphous SiO_2.[28] EELS spectra showed peaks at 10.3, 12.0, 13.8, 17.0, and 20.5 eV related to valence-electron interband excitations.[22] They are close to the positions 10.3, 11.4, 14.2, and 17.0 eV of the leading peaks in the optical conductivity of α-quartz.[60] Although a one-to-one correspondence between calculated absorption peaks and positions of structures in reflectivity and energy-loss spectra cannot be achieved, the overall agreement in the energy range of the characteristic interband energies roughly indicates the same absorption behavior versus photon energy. This justifies the inclusion of the quasiparticle aspect into the calculations.

IV. CONCLUSIONS

We present detailed parameter-free calculations of electronic structures, optical properties, and structural parameters for the three SiO_2 β-cristobalite modifications with space groups $Fd3m$, $I\bar{4}2d$, and $P2_13$. The band structures have been calculated including the excitation aspect by adding

quasiparticle shifts to the Kohn-Sham eigenvalues. The quasiparticle effects increase not only the energy gaps, but also the energy differences between states located at chemically different valence bands. We found an overall agreement of the quasiparticle energy values with the measurements to determine the valence-band states of amorphous or polycrystalline SiO_2. This holds for the fundamental gaps, the valence-band widths as well as the gaps between valence bands.

The dielectric functions of the three SiO_2 modifications have been computed within the framework of the independent-particle and independent-quasiparticle approaches. Their real parts allow the derivation of the static electronic dielectric constants. Differences in the dielectric constants could be related to the different positions of the oxygen atoms in the three modifications considered. At first sight, the dielectric constants increase when the average Si-O-Si bond angles increase. Within the independent-particle framework the calculated values approach the experimental value for β-cristobalite. According to the calculated optical absorption spectra, energy transitions whose energies are close to the fundamental gap energy have vanishing intensity. In the energy interval of 13–20 eV, our calculations reveal strong interband transitions in agreement to what has been observed by optical and electron-energy-loss spectroscopies for amorphous SiO_2 and quartz. Apart from strong excitonic resonances, the quasiparticle theory is able to reproduce important features in the optical spectra of insulating oxides such as SiO_2 in β-cristobalite form.

ACKNOWLEDGMENTS

The authors would like to thank the European Commission's 5th Framework Improving Human Potential and the Socio-Economic Knowledge Base (IHP) program for financial support in the NANOPHASE Research Training Network (Contract No. HPRN-CT-2000-00167). Part of the calculations were performed at John von Neumann Institut für Computing (NIC), Jülich, Germany (Project No. HJN21, 2003).

[1] M.K. Weldon, K.T. Queeney, J. Eng, Jr., K. Raghavachari, Y.J. Chabal, Surf. Sci. **500**, 859 (2002).
[2] F.J. Himpsel, F.R. McFeely, A. Taleb-Ibrahimi, J.A. Yarmoff, and G. Hollinger, Phys. Rev. B **38**, 6084 (1988).
[3] J. Albohn, W. Füssel, N.D. Sinh, K. Kliefoth, and W. Fuhs, J. Appl. Phys. **88**, 842 (2000).
[4] W. Orellana, A.J.R. da Silva, and A. Fazzio, Phys. Rev. Lett. **90**, 016103 (2003).
[5] P.S. Peercy, Nature (London) **406**, 1023 (2000).
[6] M.V. Wolkin, J. Jorne, P.M. Fauchet, G. Allan, and C. Delerue, Phys. Rev. Lett. **82**, 197 (1999).
[7] K.D. Hirschman, L. Tsybeskov, S.P. Duttagupta, and P.M. Fauchet, Nature (London) **384**, 338 (1996).
[8] L. Pavesi, L. Dal Negro, C. Mazzoleni, G. Franzo, and F. Friolo, Nature (London) **408**, 440 (2000).
[9] T. Demuth, Y. Jeanvoine, J. Hafner, and J.G. Ángyán, J. Phys.: Condens. Matter **11**, 3833 (1999).
[10] J.R. Chelikowsky and M. Schlüter, Phys. Rev. B **15**, 4020 (1971).
[11] P.M. Schneider and W.B. Fowler, Phys. Rev. B **18**, 7122 (1978).
[12] J.K. Rudra and W.B. Fowler, Phys. Rev. B **28**, 1061 (1983).
[13] Y.P. Li and W.Y. Ching, Phys. Rev. B **31**, 2172 (1985).
[14] S. Tsuneyuki, M. Tsukada, H. Aoki, and Y. Matsui, Phys. Rev. Lett. **61**, 869 (1988).
[15] Y.-N. Xu and W.Y. Ching, Phys. Rev. B **44**, 11 048 (1991).
[16] F. Liu, S.H. Garofalini, R.D. King-Smith, and D. Vanderbilt, Phys. Rev. Lett. **70**, 2750 (1993).
[17] I.P. Swainson and M.T. Dove, Phys. Rev. Lett. **71**, 3610 (1993).
[18] D.M. Teter, G.V. Gibbs, M.B. Boisen, Jr., D.C. Allan, and M.P. Teter, Phys. Rev. B **52**, 8064 (1995).
[19] F. Mauri, A. Pasquarello, B.G. Pfrommer, Y.-G. Yoon, and S.G. Louie, Phys. Rev. B **62**, R4786 (2000).
[20] H.R. Phillip, J. Phys. Chem. Solids **32**, 1935 (1971).
[21] T.H. DiStefano and D.E. Eastman, Phys. Rev. Lett. **27**, 1560 (1971).
[22] H. Ibach and J.E. Rowe, Phys. Rev. B **10**, 710 (1974).
[23] A. Koma and R. Ludeke, Phys. Rev. Lett. **35**, 107 (1975).
[24] B. Fischer, R.A. Pollak, T.H. DiStefano, and W.D. Grobman, Phys. Rev. B **15**, 3193 (1977).
[25] Z.A. Weinberg, G.W. Rubloff, and E. Bassous, Phys. Rev. B **19**, 3107 (1979).
[26] R.B. Laughlin, Phys. Rev. B **22**, 3021 (1980).
[27] M. Rossinelli and M.A. Bösch, Phys. Rev. B **25**, 6482 (1982).
[28] V.J. Nithianandam and S.E. Schnatterly, Phys. Rev. B **38**, 5547 (1988).
[29] S. Pantelides and W.A. Harrison, Phys. Rev. B **13**, 2667 (1976).
[30] S. Ciraci and I.P. Batra, Phys. Rev. B **15**, 4923 (1977).
[31] H. Kageshima and K. Shiraishi, Surf. Sci. **380**, 61 (1997).
[32] N. Capron, G. Boureau, A. Pasturel, and J. Hafner, J. Chem. **117**, 1843 (2002).
[33] P. Carrier, L.J. Lewis, and M.W.C. Dharma-wardana, Phys. Rev. B **64**, 195330 (2002).
[34] M. Hane, Y. Miyamoto, and A. Oshiyama, Phys. Rev. B **41**, 12 637 (1990).
[35] M. O'Keeffe and B.G. Hyde, Acta Crystallogr., Sect. B: Struct. Crystallogr. Cryst. Chem. **32**, 2923 (1976).
[36] E.K. Chang, M. Rohlfing, and S.G. Louie, Phys. Rev. Lett. **85**, 2613 (2000).
[37] P. Hohenberg and W. Kohn, Phys. Rev. **136**, B864 (1964).
[38] W. Kohn and L.J. Sham, Phys. Rev. **140**, A1139 (1965).
[39] J.P. Perdew and A. Zunger, Phys. Rev. B **23**, 5048 (1981).
[40] D.M. Ceperley and B.J. Alder, Phys. Rev. Lett. **45**, 566 (1980).
[41] G. Kresse and J. Furthmüller, Comput. Mater. Sci. **6**, 15 (1996).
[42] G. Kresse and J. Furthmüller, Phys. Rev. B **54**, 11 169 (1996).
[43] P.E. Blöchl, Phys. Rev. B **50**, 17 953 (1994).
[44] G. Kresse and D. Joubert, Phys. Rev. B **59**, 1758 (1999).
[45] B. Adolph, J. Furthmüller, and F. Bechstedt, Phys. Rev. B **63**, 125108 (2001).
[46] J. Furthmüller, G. Cappellini, H.-Ch. Weissker, and F. Bechstedt, Phys. Rev. B **66**, 045110 (2002).

[47] G. Onida, L. Reining, and A. Rubio, Rev. Mod. Phys. **74**, 601 (2002).
[48] D. Vanderbilt, Phys. Rev. B **41**, 7892 (1990).
[49] J. Furthmüller, P. Käckell, F. Bechstedt, and G. Kresse, Phys. Rev. B **61**, 4576 (2000).
[50] F.D. Murnaghan, Proc. Natl. Acad. Sci. U.S.A. **30**, 244 (1944).
[51] M.S. Hybertsen and S.G. Louie, Phys. Rev. B **34**, 5390 (1986).
[52] R.W. Godby, M. Schlüter, and L.J. Sham, Phys. Rev. B **37**, 10 159 (1988).
[53] F. Bechstedt, R. Del Sole, G. Cappellini, and L. Reining, Solid State Commun. **84**, 765 (1992); G. Cappellini, R. Del Sole, L. Reining, and F. Bechstedt, Phys. Rev. B **47**, 9892 (1993).
[54] B. Adolph, V.I. Gavrilenko, K. Tenelsen, F. Bechstedt, and R. Del Sole, Phys. Rev. B **53**, 9797 (1996).
[55] H. Kageshima and K. Shiraishi, Phys. Rev. B **56**, 14 985 (1997).
[56] R. DelSole and R. Girlanda, Phys. Rev. B **48**, 11 789 (1993).
[57] Z.H. Levine and D.C. Allan, Phys. Rev. Lett. **63**, 1719 (1989).
[58] H.J. Monkhorst and J.D. Pack, Phys. Rev. B **13**, 5188 (1976).
[59] F. Bechstedt and R. Del Sole, Phys. Rev. B **38**, 7710 (1988).
[60] H.R. Phillip, in *Handbook of Optical Constants of Solids*, edited by E.D. Palik (Academic, Orlando, FL, 1985), p. 719.
[61] W.G. Schmidt, J.L. Fattebert, J. Bernholc, and F. Bechstedt, Surf. Rev. Lett. **6**, 1159 (1999).